ISSN 0915-633X

NATIONAL INSTITUTE FOR FUSION SCIENCE

Structure Formation of a Single Polymer Chain. I: Growth of trans Domains

S. Fujiwara and T. Sato

(Received - Oct. 20, 2000)

NIFS-665 Nov. 2000

RESEARCH REPORT
NIFS Series

TOKI, JAPAN

Structure formation of a single polymer chain. I: Growth of *trans* domains

Susumu Fujiwara and Tetsuya Sato

Theory and Computer Simulation Center, National Institute for Fusion Science, 322-6 Oroshi-cho, Toki-shi 509-5292, Japan

Abstract

Molecular dynamics simulations are carried out to study structure formation of a single polymer chain with 500 CH_2 groups. Our simulations show that the orientationally ordered structure is formed at a low temperature both by gradual stepwise cooling and by quenching from a random configuration at a higher temperature. The growth of the global orientational order proceeds *in a gradual manner* in the case of gradual stepwise cooling, whereas it proceeds *in a stepwise manner* in the case of quenching. From the microscopic analysis of the structure formation process, we find the following characteristic features: (i) In the case of gradual stepwise cooling, the global orientational order grows gradually through the incorporation of small *trans* domains and the surrounding *trans* segments into the largest *trans* domain. (ii) In the case of quenching, the growth of the orientational order is either due to the incorporation of small *trans* domains and the surrounding *trans* segments into the largest *trans* domain or due to the elongation of the *trans* segments in the largest *trans* domain. The last feature endorses the previously proposed hypothetical grand view of self-organization [e.g. T. Sato, Phys. Plasmas **3**, 2135 (1996)]: when a system is driven far from equilibrium, it will evolve to a more stable state in a stepwise fashion irrespective of its fundamental interaction forces.

Keywords: molecular dynamics simulation, polymer chain,structure formation, orientational order, *trans* domain

1 Introduction

Structure formation or self-organization of chain molecules, such as n-alkanes, polyethylene chains and lipid molecules, has recently become the focus of attention in physics, chemistry, biology, and material science. The crystal structure of the rotator phase of n-alkanes has been extensively studied by several experimental techniques including x-ray diffraction [1–4], infrared and Raman spectroscopy [5, 6], neutron scattering [7, 8], and NMR [9]. The primary nucleation in the crystallization induction period of polyethylene [10–12] and poly(ethylene terephthalate) [13–18] has been investigated by various time-resolved measurements. The morphologies of the self-assembled aggregates formed by the association of lipid molecules in solution, such as spherical micelles, cylindrical micelles, and lipid bilayers, have been experimentally studied [19–21]. Although numerous experimental investigations have thus been made on the structure formation of chain molecules, little is known about the detailed mechanisms of the structure formation of chain molecules *at the molecular level*.

Computer simulation is one of the powerful tools for investigating the mechanisms of structure formation process at the molecular level. Over the last decade, several molecular dynamics (MD) simulations have been performed on structure formation of an isolated single polymer chain in order to examine the primary nucleation process [22–26]. Kavassalis *et al.* carried out MD simulations of the folding process of a polyethylene chain from an all-*trans* conformation and rotational isomeric state conformation below the equilibrium melting temperature [22, 23]. Fujiwara *et al.* studied the formation process of the orientationally ordered structure of a single polymer chain from a random configuration by gradual stepwise cooling [24]. The relaxation of a fully extended polyethylene chain was investigated by Liao *et al.* [25]. They found that the relaxation proceeds in three stages when a chain has more than 1200 methylene groups. Iwata *et al.* performed MD simulations on the melting and crystallization processes of a single polymer chain and analysed chain movement in the crystallization process [26]. Computer simulation has also been done on the coil-globule transition [27–30] and the relaxation [31, 32] of

an isolated single polymer chain. The thermodynamics of an isolated single homopolymer chain has been investigated using a lattice Monte Carlo (MC) simulation [27] and an off-lattice MC simulation [28–30]. The relaxation modes and rates of a single polymer chain have been studied by MC simulations [31] and MD simulations [32].

The purpose of this paper is to clarify the mechanisms of structure formation of polymer chains *at the molecular level*. In particular, our concern is to investigate the structure formation process of a single polymer chain by cooling. To this end, we carry out the MD simulations of a single polymer chain and analyze the formation process of the orientationally ordered structure during gradual stepwise cooling and during quenching.

In our previous paper [24], we investigated the global orientational order and the conformational defects of a single polymer chain during gradual stepwise cooling. It was found from our previous simulations that the orientationally ordered structure was formed from a random configuration by a gradual stepwise cooling and the global orientational order grew below $T = 550$ K. In this series of papers, we first discuss the growth process of *trans* domains which physically mean bunches of local orientationally-ordered *trans* segments. In the subsequent paper, we will investigate structure and molecular motion during the structure formation process. This paper is organized as follows. In Sec. 2 we give a detailed description of our simulation model and method. Our simulation results by gradual stepwise cooling are presented in Sec. 3 and those by quenching in Sec. 4. Summary and discussion are given in Sec. 5.

2 Model and Method

The present computational model is the same as that used in the previous work on the structure formation of a single polymer chain [24]. The model polymer chain consists of a sequence of methylene (CH_2) groups, which are treated as united atoms. The mass of each methylene group is 14 g/mol. The united atoms interact via bonded potentials (bond-stretching, bond-bending, and torsional potentials) and a non-bonded potential (12-6 Lennard-Jones potential). The atomic force field used here is the DREIDING potential [33]: (i) the bond-stretching potential,

$$V_{\rm stretch}(d) = \frac{1}{2}k_{\rm d}(d - d_0)^2, \qquad (1)$$

where d_0 is the equilibrium bond length and d is the actual bond length, (ii) the bond-bending potential,

$$V_{\rm bend}(\theta) = \frac{1}{2}k_\theta(\theta - \theta_0)^2, \qquad (2)$$

where θ_0 is the equilibrium bond angle and θ is the bond angle between three adjacent atoms, (iii) the torsional potential,

$$V_{\rm torsion}(\phi) = \frac{1}{2}k_\phi[1 - \cos(3\phi)], \qquad (3)$$

where ϕ is the dihedral angle formed by four consecutive atoms, and (iv) the 12-6 Lennard-Jones potential between atoms separated by more than two bonds,

$$V_{\rm LJ}(r) = 4\epsilon\left[\left(\frac{\sigma}{r}\right)^{12} - \left(\frac{\sigma}{r}\right)^{6}\right], \qquad (4)$$

where r is the distance between atoms. The values of all the potential parameters are listed in Table 1.

The equations of motion for all atoms are solved numerically using the velocity Verlet algorithm [34] and apply the Nosé-Hoover method in order to keep the temperature of the system constant [35–37]. The integration time step and the relaxation constant for the heat bath variable are 1.0 fs and 0.1 ps, respectively. The cutoff distance for the 12-6 Lennard-Jones potential is 10.5 Å. A single polymer chain with 500 methylene groups is exposed to vacuum and other molecules such as solvent molecules are not considered. The total linear momentum and angular momentum are set to be zero in order to cancel overall translation and rotation of a polymer chain. The MD simulations are carried out as follows. At first, we provide a random configuration of a single polymer chain with 500 united atoms at high temperature ($T = 800$ K). The system is then cooled to lower temperature by the following cooling manners: (i) **Gradual stepwise cooling**. The system is cooled stepwise to $T = 100$ K with the rate of 50 K/1 ns and a simulation of 1 ns (1×10^6 time steps) is carried out at each temperature [Fig. 1(a)]. (ii) **Quenching**. The system is quenched to a lower temperature and simulations of 15 ns (1.5×10^7 time steps) are carried out for several quenching temperatures ($T = 200, 250, \ldots, 550$ K) [Fig. 1(b)].

In the following sections, we describe, in detail, our simulation results by gradual stepwise cooling (Sec. 3) and by quenching (Sec. 4).

3 Structure Formation by Gradual Stepwise Cooling

3.1 Formation process of global orientational order

In this subsection, we analyze the chain configuration and the global orientational order in the process of structure formation by gradual stepwise cooling.

3.1.1 Chain configuration

Snapshots of the final chain configuration at various temperatures ($T = 800$, 500, 400, and 100 K) are shown in Fig. 2. Here we introduce the coordinate system with three principal axes of inertia of a single polymer chain. In this coordinate system, the origin is

located at the center-of-mass position, the x-axis is the principal axis with the largest moment of inertia and the z-axis is that with the smallest moment of inertia. In this figure, top and bottom snapshots are respectively viewed along the z-axis (top view) and along the direction perpendicular to the z-axis (side view). Figure 2 indicates the following features: (i) At high temperature (T = 800 K), *gauche* states are excited everywhere and a polymer chain takes a random configuration. (ii) At lower temperature ($T \leq 400$ K), the orientationally ordered structure is formed by gradual stepwise cooling and the global change of the chain conformation is not recognized. (iii) In the orientationally ordered structure, the *gauche* excitations are located exclusively in the fold surfaces.

3.1.2 Global orientational order parameter

In order to investigate the growth process of the global orientational order, we calculate the global orientational order parameter P_2, which is defined by

$$P_2 = \left\langle \frac{3\cos^2\psi - 1}{2} \right\rangle_{\text{bond}}, \tag{5}$$

where ψ is the angle between two chord vectors and $\langle\cdots\rangle_{\text{bond}}$ denotes the average over all pairs of chord vectors. The chord vector is defined as the vector formed by connecting centers of two adjacent bonds along the polymer chain. The parameter P_2 takes a value of 1.0 when all chord vectors are parallel and that of 0.0 when chord vectors are randomly oriented. The temperature dependence of the global orientational order parameter P_2 is plotted in Fig. 3. The time average is taken during the last 0.8 ns for each temperature. The following features are found from this figure: (i) At high temperature above T = 550 K, the parameter P_2 takes a value near zero, which shows that there exists no global orientational order in this temperature region. (ii) At lower temperature than T = 550 K, P_2 increases as the temperature decreases, which indicates that the global orientational order starts to grow below T = 550 K. (iii) At lower temperature than T = 350 K, the growth rate of the orientational order becomes small The reason for this is that, in this temperature region, the global conformational change of the polymer chain ceases and only the local motion of united atoms with no global change takes place.

We show, in Fig. 4, the time dependence of the global orientational order parameter P_2 for various temperatures using the segmental average with Δt = 5 ps. At $T \geq 550$ K, the parameter P_2 is smaller than 0.1, that is, there exists no global orientational order [Figs. 4(a) and 4(b)]. At T = 500 K and T = 450 K, P_2 fluctuates greatly between 0.1 and 0.3 [Figs. 4(c) and 4(d)]. When the temperature is T = 400 K, the parameter P_2 fluctuates between 0.1 and 0.3 up to $t \approx 0.35$ ns and it gradually increases to 0.4 afterwards [Fig. 4(e)]. This indicates that the global orientational order grows *in a gradual manner* in the case of gradual stepwise cooling. At T = 350 K, P_2 has a nearly-constant value of 0.42 with minor fluctuation [Fig. 4(f)].

3.2 Microscopic analysis of the structure formation process

In this subsection, we first examine the conformational change and then analyze the parallel ordering process in order to investigate, at the molecular level, the structure formation process by gradual stepwise cooling.

3.2.1 Conformational change

In order to investigate the conformational change, we examine the stretching of chain molecules. We define the *trans* state and the *gauche* state by $|\phi| \leq \pi/3$ and $|\phi| > \pi/3$, respectively, where ϕ is the dihedral angle. We calculate the distribution of the size of the *trans* segments, i.e., the number of consecutive *trans* bonds, n_{tr}. The distribution of the size of the *trans* segments $P(n_{\text{tr}})$ is normalized as

$$\sum_{n_{\text{tr}}=1}^{N-3} P(n_{\text{tr}}) = 1, \tag{6}$$

where N is the number of atoms in a polymer chain (N = 500 in this work). The distribution $P(n_{\text{tr}})$ is shown in Fig. 5 at various temperatures. The time average is taken during the last 50 ps for each temperature. At T = 800 K, $P(n_{\text{tr}})$ decreases exponentially with the increase of the size n_{tr} [Inset of Fig. 5(a)]. The reason for this exponential decrease is that, at high temperature, each bond takes the *trans* state or the *gauche* state randomly, that is, there is no spatial correlation between the *trans* state and the *gauche* state. At T = 500 K, the fraction of the small *trans* segments with $n_{\text{tr}} < 10$ decreases while that of the large *trans* segments with $n_{\text{tr}} > 10$ increases [Fig. 5(b)]. As shown in Figs. 5(c) and 5(d), a flat region appears between n_{tr} = 10 and n_{tr} = 20 at T = 450 K and extends to n_{tr} = 25 at T = 400 K. When the temperature is reduced to T = 350 K, the flat region disappears and another peak becomes visible around n_{tr} = 24, which results in a bimodal distribution [Fig. 5(e)]. At T = 100 K, we can see two peaks around n_{tr} = 2 and n_{tr} = 25 which are completely separated. This suggests that the orientationally ordered structure consists of two parts: fold surface and stem region. A peak around n_{tr} = 2 corresponds to the *trans* segments in the fold surfaces and another peak around n_{tr} = 25 corresponds to those in the stem region.

We show, in Fig. 6, the average size of the *trans* segments, $\overline{n_{\text{tr}}}$, which is defined by

$$\overline{n_{\text{tr}}} = \sum_{n_{\text{tr}}=1}^{N-3} n_{\text{tr}} P(n_{\text{tr}}) \tag{7}$$

and satisfies $1 \leq \overline{n_{\text{tr}}} \leq N - 3 (= 497)$, as a function of the inverse temperature. The time average is taken

during the last 0.8 ns for each temperature. The average size of the *trans* segments $\overline{n_{\rm tr}}$ corresponds to the persistence length, which should satisfy the following relation at high temperature [38]:

$$\overline{n_{\rm tr}} \propto \exp\left(\frac{\Delta\varepsilon}{k_{\rm B}T}\right), \tag{8}$$

where $\Delta\varepsilon$ is the torsional energy difference between the *trans* and the *gauche* conformations and $k_{\rm B}$ is the Boltzmann constant. As can be seen from Fig. 6, the data at high temperature ($T \geq 400$ K) are well fitted by Eq. (8) and the fitting parameter $\Delta\varepsilon/k_{\rm B}$ is estimated as $\Delta\varepsilon/k_{\rm B} \approx 1.88$ (kcal/mol). At low temperature of $T < 400$ K, on the other hand, the average size $\overline{n_{\rm tr}}$ is almost constant because of the formation of the orientationally ordered structure.

3.2.2 Parallel ordering

We investigate, in this subsection, the parallel ordering process. In order to measure the extent of the local orientational order, we need introduce the concept of a "*trans* domain", which will physically mean a bunch of local orientationally-ordered *trans* segments which is formed through parallel ordering. The *trans* domain is an expansion of a "domain" defined in the context of short chain-molecule systems [39–42]. Our precise definition of a *trans* domain is as follows. Two *trans* segments, i and j, belong to the same *trans* domain if the following three conditions are satisfied:

$$\begin{cases} \text{(i)} & \min\limits_{k,l} |\mathbf{r}_k^i - \mathbf{r}_l^j| < r_0, \\ \text{(ii)} & \min\limits_k \left(\hat{\mathbf{u}}_i \cdot \mathbf{r}_k^i\right) < \hat{\mathbf{u}}_i \cdot \mathbf{r}_c^j < \max\limits_k \left(\hat{\mathbf{u}}_i \cdot \mathbf{r}_k^i\right) \\ & \qquad\qquad \text{or} \\ & \min\limits_k \left(\hat{\mathbf{u}}_j \cdot \mathbf{r}_k^j\right) < \hat{\mathbf{u}}_j \cdot \mathbf{r}_c^i < \max\limits_k \left(\hat{\mathbf{u}}_j \cdot \mathbf{r}_k^j\right), \\ \text{(iii)} & \alpha_{ij} < \alpha_0, \end{cases}$$

where $\mathbf{r}_k^i$ is the position vector of the k-th atom in the i-th *trans* segment, $\hat{\mathbf{u}}_i$ is the unit vector directed along the principal axis with the smallest moment of inertia of the i-th *trans* segment, $\mathbf{r}_c^i$ is the position vector of the center of mass of the i-th *trans* segment, and α_{ij}, which satisfies $0 \leq \alpha_{ij} \leq \pi/2$, is the angle between the principal axis with the smallest moment of inertia of the i-th *trans* segment and that of the j-th *trans* segment. The first condition means that the shortest distance, d_{ij}, between two *trans* segments is relatively short [Fig. 7(a)]. The second condition indicates that the foot of a perpendicular drawn from the center of mass of the j-th *trans* segment to the i-th *trans* segment, P_{ij}, stands on the i-th *trans* segment, or vice versa [Fig. 7(a)]. Under this condition, two *trans* segments shown in Fig. 7(b) do not belong to the same *trans* domain. The last condition represents that the directions of two *trans* segments are almost parallel. In our calculations, we set $r_0 = 1.5\sigma$ and $\alpha_0 = 10°$. We show, in Fig. 8, the time evolution of the largest *trans* domain size s at various temperatures using the segmental average with $\Delta t = 5$ ps. At $T \geq 550$ K, only small *trans* domains whose sizes are smaller than 50 can be observed [Figs. 8(a) and 8(b)]. At $T = 500$ K and $T = 450$ K, the largest *trans* domain size s fluctuates greatly between 50 and 200, and between 50 and 300, respectively [Figs. 8(c) and 8(d)]. When the temperature is $T = 400$ K, s gradually increases with the elapse of time and reaches about 300 at $t \approx 0.7$ ns [Fig. 8(e)]. This result, together with the result in Sec. 3.1.2, leads to the conclusion that both the global orientational order and the local orientational order grow *in a gradual manner* in the case of gradual stepwise cooling. At $T = 350$ K, s fluctuates between 200 and 400 [Fig. 8(f)].

We then calculate the number of *trans* segments in the largest *trans* domain, $n_{(1)}$, and the average *trans* segment size in the largest *trans* domain, $\overline{n_{\rm tr}^{(1)}}$, in order to investigate the growth process of *trans* domains in detail. Note that the relation $s = n^{(1)} \times \overline{n_{\rm tr}^{(1)}}$ holds. The time evolution of P_2, s, $n^{(1)}$, and $\overline{n_{\rm tr}^{(1)}}$ at $T = 400$ K is plotted using the segmental average with $\Delta t = 5$ ps in Fig. 9. From this figure, we find the following features: (i) At $T = 400$ K, both the global orientational order and the local orientational order grow in a gradual manner [Figs. 9(a) and 9(b)]. (ii) The number of *trans* segments in the largest *trans* domain, $n_{(1)}$, increases more markedly than the average *trans* segment size in the largest *trans* domain, $\overline{n_{\rm tr}^{(1)}}$ [Figs. 9(c) and 9(d)]. This fact indicates that the growth of the orientational order is mainly due to the increase of $n_{(1)}$, that is, the orientational order grows through the incorporation of small *trans* domains and the surrounding *trans* segments into the largest *trans* domain.

We show *trans* domains at $t = 0.3$, 0.6, and 0.9 ns for $T = 400$ K in Fig. 10 in order to see the growth process of *trans* domains. Three *trans* domains (red, blue, and yellow), whose sizes are larger than 30, are observed at $t = 0.3$ ns [Fig. 10(A)]. Figures 10(B) and 10(C) tell us that small *trans* domains and the surrounding *trans* segments are incorporated into the largest *trans* domain as time advances. It is also found that the largest *trans* domain is situated in the stem region and small *trans* segments and the *gauche* bonds are located mainly in the fold surfaces [Fig. 10(C)].

4 Structure Formation by Quenching

4.1 Formation process of global orientational order

In this subsection, we analyze the chain configuration and the global orientational order in the process of structure formation by quenching.

4.1.1 Chain configuration

Snapshots of the final chain configuration at various low temperatures (T = 400, 350, 300, and 250 K) are shown in Fig. 11. This figure shows the following features: (i) The stem length becomes shorter as the temperature decreases. (ii) The *gauche* excitations are located chiefly in the fold surfaces as in the case of gradual stepwise cooling.

4.1.2 Global orientational order parameter

We then calculate the global orientational order parameter P_2 defined by Eq. (5). The temperature dependence of the global orientational order parameter P_2 is shown in Fig. 12 in the case of quenching. The time average is taken during the last 10 ns for each temperature. This figure tells us the following features: (i) At high temperature above T = 500 K, the parameter P_2 takes a value below 0.2, which means that the global orientation is almost random in this temperature region. (ii) At lower temperature than T = 500 K, P_2 increases with the decrease of temperature as in the case of gradual stepwise cooling (Sec. 3.1.2). (iii) At lower temperature than T = 400 K, P_2 decreases gradually as the temperature decreases, which is in marked contrast to the temperature dependence of P_2 in the case of gradual stepwise cooling (Sec. 3.1.2). This temperature dependence is probably caused by the fact that the polymer chain is easy to be trapped in the metastable state at lower temperature.

We show, in Fig. 13, the time dependence of the global orientational order parameter P_2 for various temperatures using the segmental average with Δt = 20 ps in the case of quenching. At T = 500 K, we can see the clear transition between the orientationally ordered state ($P_2 > 0.2$) and the randomly oriented state ($P_2 < 0.1$) [Fig. 13(a)]. The similar transition can be observed also at T = 450 K [Fig. 13(b)]. At T = 400 K, the parameter P_2 gradually increases up to $t \approx 2.3$ ns and is almost constant afterwards [Fig. 13(c)]. When the temperature is T = 350 K, P_2 takes a value smaller than 0.2 up to $t \approx 2.5$ ns. The parameter P_2 increases sharply at $t \approx 2.5$ ns and reaches about 0.4 at $t \approx 3.5$ ns [Fig. 13(d)]. The similar stepwise growth of the global orientational order can also be seen at $t \approx 11$ ns for T = 300 K and at $t \approx 7.8$ ns for T = 250 K [Figs. 13(e) and 13(f)]. This fact indicates that the global orientational order grows *in a stepwise manner* at lower temperature in the case of quenching, which exhibits a striking contrast to the growth manner of the global orientational order in the case of gradual stepwise cooling (Sec. 3.1.2). As we shall see later (Sec. 4.2.2), the main cause of the stepwise increase of P_2 at T = 300 K differs from that at T = 250 K.

4.2 Microscopic analysis of the structure formation process

In this subsection, we first examine the conformational change and then analyze the parallel ordering process at the molecular level during structure formation by quenching.

4.2.1 Conformational change

The distribution of the size of the *trans* segments $P(n_{\rm tr})$ is shown in Fig. 14 at various temperatures The time average is taken during the last 1 ns for each temperature. At T = 500 K, $P(n_{\rm tr})$ decreases monotonically with the increase of the size $n_{\rm tr}$ [Fig. 14(a)]. At T = 450 K, a flat region appears between $n_{\rm tr}$ = 10 and $n_{\rm tr}$ = 20 [Fig. 14(b)]. At $T \leq 400$ K, the distribution becomes bimodal [Figs. 14(c)-14(f)]. It is found from Figs. 14(c)-14(f) that the second peak position around $n_{\rm tr}$ = 20 becomes smaller as the temperature is reduced. This fact means that, as observed above (Sec. 4.1.1), the stem length becomes shorter as the temperature decreases because the second peak corresponds to the *trans* segments in the stem region.

The average size of the *trans* segments $\overline{n_{\rm tr}}$ is plotted in Fig. 15. The time average is taken during the last 10 ns for each temperature. It is found from this figure that the data at $T \geq 400$ K are well fitted by Eq. (8) with the fitting parameter $\Delta\varepsilon/k_{\rm B} \approx 1.88$ (kcal/mol). On the other hand, the average size $\overline{n_{\rm tr}}$ is almost constant at $T < 400$ K. These features are also seen in the case of gradual stepwise cooling (Sec. 3.2.1).

4.2.2 Parallel ordering

In this subsection, we study the parallel ordering process. We show, in Fig. 16, the time evolution of the largest *trans* domain size s at various temperatures using the segmental average with Δt = 20 ps. At $T \geq 450$ K [Figs. 16(a) and 16(b)], the largest *trans* domain size s fluctuates greatly in accordance with the temporal behavior of the global orientational order parameter P_2 [Figs. 13(a) and 13(b)]. When the temperature is T = 400 K, s gradually increases with the elapse of time, reaches about 370 at $t \approx 2.3$ ns and fluctuates between 300 and 400 afterwards [Fig. 16(c)]. At T = 350 K [Fig. 16(d)], only small *trans* domains whose sizes are smaller than 100 can be seen up to $t \approx 2.5$ ns. The largest *trans* domain s sharply increases at $t \approx 2.5$ ns and reaches about 350 at $t \approx 3.5$ ns. The similar stepwise growth of the largest *trans* domain size can also be observed at $t \approx 11$ ns for T = 300 K [Fig. 16(e)]. At T = 250 K, a clear change in the largest *trans* domain size cannot be recognized at $t \approx 7.8$ ns [Fig. 16(f)] while the stepwise growth of the global orientational order can be observed at $t \approx 7.8$ ns [Fig. 13(f)].

We show the time evolution of P_2, s, $n^{(1)}$, and $\overline{n_{\rm tr}^{(1)}}$ at T = 300 K and T = 250 K using the segmental average with Δt = 20 ps in Figs. 17 and 18, respectively. Figure 17 tells us that, at T = 300 K,

both the global orientational order and the local orientational order grow in a stepwise fashion at $t \approx 11$ ns [Figs. 17(a) and 17(b)]. It is found from Fig. 17 that the growth of the orientational order is due to the increase of $n_{(1)}$ as in the case of gradual stepwise cooling (Fig. 9). It is ascertained that the stepwise growth of the orientational order at $T = 350$ K is also due to the stepwise increase of $n_{(1)}$. From Fig. 18, we find the following features at $T = 250$ K: (i) The global orientational order parameter P_2 increases sharply at $t \approx 7.8$ ns [Fig. 18(a)]. On the other hand, a marked change in the largest *trans* domain size s cannot be observed at $t \approx 7.8$ ns [Fig. 18(a)]. (ii) The growth of the global orientational order is due to the increase of the average *trans* segment size in the largest *trans* domain, $\overline{n_{\rm tr}^{(1)}}$. This means that, at $T = 250$ K, the growth of the orientational order is not caused by the incorporation of small *trans* domains and the surrounding *trans* segments into the largest *trans* domain but by the elongation of the *trans* segments in the largest *trans* domain.

We show *trans* domains at $t = 11.0$, 11.2, and 11.3 ns for $T = 300$ K and at $t = 7.7$, 7.83, and 8.0 ns for $T = 250$ K in Figs. 19 and 20, respectively. At $T = 300$ K, there are three *trans* domains (red, blue, and yellow), whose sizes are larger than 30, at $t = 11.0$ ns [Fig. 19(A)]. As time elapses, small *trans* domains and the surrounding *trans* segments are incorporated into the largest *trans* domain [Figs. 19(B) and 19(C)]. As a result, the number of *trans* segments in the largest *trans* domain increases. At $T = 250$ K, on the other hand, an overall *trans* domain is located in the stem region at $t = 7.7$ ns [Fig. 20(A)] and the average length of the *trans* segments in the largest *trans* domain becomes longer with the elapse of time [Figs. 20(B) and 20(C)].

5 Summary and Discussion

In this paper, we have carried out MD simulation of a single polymer chain with 500 methylene groups. By investigating the growth process of the global orientational order and making a microscopic analysis of the structure formation process, the following results have been obtained:

(i) The orientationally ordered structure is formed at a low temperature by gradual stepwise cooling or by quenching from a random configuration at a higher temperature.

(ii) The global orientational order grows *in a gradual manner* in the case of gradual stepwise cooling, whereas it grows *in a stepwise manner* in the case of quenching.

(iii) In the case of gradual stepwise cooling, the global orientational order starts to grow at $T = 550$ K and the orientationally ordered structure is formed at $T = 400$ K. At $T = 400$ K, the global orientational order grows gradually through the incorporation of small *trans* domains and the surrounding *trans* segments into the largest *trans* domain.

(iv) In the case of quenching, the orientationally ordered structure is formed at $T \leq 400$ K. At $T \leq 400$ K, the global orientational order grows in a stepwise fashion in contrast to the case of gradual stepwise cooling. The growth of the orientational order is mainly due to the incorporation of small *trans* domains and the surrounding *trans* segments into the largest *trans* domain at $T = 350$ and $T = 300$ K, whereas it is caused by the elongation of the *trans* segments in the largest *trans* domain at $T = 250$ K.

The result that the global orientational order grows in a stepwise fashion in the case of quenching can be interpreted in the following way. In the case of quenching, the system tends to be trapped in a metastable state which corresponds to less orientationally-ordered structure and stays in the metastable state for some duration. Once the system finds out a path to another metastable state, it makes a sudden transition from the original metastable state to another metastable state through the path.

Here we discuss structure formation of a single polymer chain from the energetic point of view. Let us imagine a polymer chain in the all-*trans* conformation. When the polymer chain folds, the Lennard-Jones potential energy, $E_{\rm LJ}$, decreases whereas the bonded potential energy, $E_{\rm b}$, increases. For the folded orientationally-ordered structure to be formed, the total potential energy, $E_{\rm tot}$, should be smaller than that of the all-*trans* conformation. In Fig. 21, we show potential energies, $E_{\rm b}$, $E_{\rm LJ}$ and $E_{\rm tot}$, as a function of temperature in the case of gradual stepwise cooling. Time average is taken during the last 0.8 ns. It is found from Fig. 21(a) that both the bonded potential energy and the Lennard-Jones potential energy decrease as the temperature decreases. Figure 21(b) tells us that the total potential energy becomes smaller than that of the all-*trans* conformation [a broken line in Fig. 21(b)] below about 400 K. This suggests that the transition into the orientationally ordered structure takes place around $T = 400$ K, which is consistent with the above third result, (iii).

Incidentally, a hypothetical grand view of self-organization is proposed by one of the authors (T. Sato) on the basis of extensive computer simulations on plasmas [43–46]. According to this grand view, when a system is driven far from equilibrium, it will evolve to a more stable state *in a stepwise fashion* irrespective of the types of particle interactions. Our simulation result that the orientational order grows *in a stepwise fashion* in the case of quenching lend support to this hypothetical grand view of self-organization.

In the subsequent paper, we will study structure and molecular motion during the structure formation process. For the future work, we will carry out MD

simulation of a single polymer chain in solution in order to investigate the effect of solvent molecules on the structure formation of a single polymer chain.

Acknowledgments

This work was partially supported by Grant-in-Aid (No. 10044105 and No. 10740199) and Grant-in-Aid for Scientific Research on Priority Areas, "Mechanism of Polymer Crystallization" (No. 12127206) from the Ministry of Education, Science, Sports and Culture. This work was carried out by using the Advanced Computing System for Complexity Simulation (NEC SX-4/64M2) at National Institute for Fusion Science.

References

[1] I. Denicolo, J. Doucet, and A.F. Craievich, J. Chem. Phys. **78**, 1465 (1983).

[2] J. Doucet, I. Denicolo, A.F. Craievich, and C. Germain, J. Chem. Phys. **80**, 1647 (1984).

[3] A.F. Craievich, I. Denicolo, and J. Doucet, Phys. Rev. B **30**, 4782 (1984).

[4] G. Ungar, J. Phys. Chem. **87**, 689 (1983).

[5] G. Zerbi, R. Magni, M. Gussoni, K.H. Moritz, A. Bigotto, and S. Dirlikov, J. Chem. Phys. **75**, 3175 (1981).

[6] M. Maroncelli, H.L. Strauss, and R.G. Snyder, J. Chem. Phys. **82**, 2811 (1985).

[7] J. Doucet and A.J. Dianoux, J. Chem. Phys. **81**, 5043 (1984).

[8] F. Guillaume, J. Doucet, C. Sourisseau, and A.J. Dianoux, J. Chem. Phys. **91**, 2555 (1989).

[9] M.G. Taylor, E.C. Kelusky, I.C.P. Smith, H.L. Casal, and D.G. Cameron, J. Chem. Phys. **78**, 5108 (1983).

[10] K. Tashiro, M. Izuchi, F. Kaneuchi, C. Jin, M. Kobayashi, and R.S. Stein, Macromolecules **27**, 1240 (1994).

[11] K. Tashiro, K. Imanishi, Y. Izumi, M. Kobayashi, K. Kobayashi, M. Satoh, and R.S. Stein, Macromolecules **28**, 8477 (1995).

[12] K. Tashiro, S. Sasaki, and M. Kobayashi, Macromolecules **29**, 7460 (1996).

[13] M. Imai, K. Kaji, and T. Kanaya, Phys. Rev. Lett. **71**, 4162 (1993).

[14] M. Imai, K. Kaji, and T. Kanaya, Macromolecules **27**, 7103 (1994).

[15] M. Imai, K. Kaji, T. Kanaya, and Y. Sakai, Physica B **213/214**, 718 (1995).

[16] M Imai, K. Kaji, T. Kanaya, and Y. Sakai, Phys Rev B **52**, 12696 (1995)

[17] K. Fukao and Y. Miyamoto, Phys. Rev Lett. **79**, 4613 (1997).

[18] K. Fukao and Y. Miyamoto, J. Non-Cryst. Solids **212**, 208 (1997).

[19] A Saitoh, K. Takiguchi, Y. Tanaka, and H. Hotani, Proc. Natl. Acad. Sci. USA **95**, 1026 (1998).

[20] R. Oda, L. Bourdieu, and M. Schmutz, J. Phys. Chem. B **101**, 5913 (1997).

[21] R. Oda, I. Huc, M. Schmutz, S.J. Candau, and F. MacKintosh, Nature **339**, 566 (1999).

[22] T.A. Kavassalis and P.R. Sundararajan, Macromolecules **26**, 4144 (1993).

[23] P.R. Sundararajan and T.A. Kavassalis, J. Chem Soc. Faraday Trans. **91**, 2541 (1995).

[24] S. Fujiwara and T. Sato, J. Chem. Phys. **107**, 613 (1997).

[25] Q. Liao and X. Jin, J. Chem. Phys. **110**, 8835 (1999).

[26] M. Iwata and H. Sato, Phys. Chem. Chem. Phys. **1**, 2491 (1999).

[27] J.P.K. Doye, R.P. Sear, and D. Frenkel, J. Chem. Phys. **108**, 2134 (1998).

[28] H. Noguchi, S. Saito. S. Kidoaki, and K. Yoshikawa, Chem. Phys. Lett. **261**, 527 (1996).

[29] H. Noguchi and K. Yoshikawa, Chem Phys. Lett. **278**, 184 (1997).

[30] H. Noguchi and K. Yoshikawa, J. Chem. Phys. **109**, 5070 (1998).

[31] S. Koseki, H Hirao, and H. Takano, J. Phys. Soc. Jpn. **66**, 1631 (1997).

[32] H. Hirao, S. Koseki, and H. Takano, J. Phys. Soc. Jpn. **66**, 3399 (1997).

[33] S.L. Mayo, B.D. Olafson, and W.A. Goddard III. J. Phys. Chem. **94**, 8897 (1990).

[34] W.C. Swope, H.C. Andersen, P.H. Berens, and K.R. Wilson, J. Chem. Phys. **76**, 637 (1982).

[35] S. Nosé, Mol. Phys. **52**, 255 (1984).

[36] S. Nosé. J. Chem. Phys. **81**, 511 (1984).

[37] W.G. Hoover, Phys. Rev. A **31**, 1695 (1985).

[38] P.G. de Gennes, *Scaling Concepts in Polymer Physics* (Cornell University Press, Ithaca, 1979).

[39] K. Esselink, P.A.J. Hilbers, and B.W.H. van Beest, J. Chem. Phys. **101**, 9033 (1994).

[40] S. Fujiwara and T. Sato, Phys. Rev. Lett. **80**, 991 (1998).

[41] S. Fujiwara and T. Sato, Mol. Simul. **21**, 271 (1999).

[42] S. Fujiwara and T. Sato, J. Plasma Fusion Res. SERIES **2**, 498 (1999).

[43] T. Sato, Phys. Plasmas **3**, 2135 (1996).

[44] T. Sato, J. Korean Phys. Soc. (Proc. Suppl.) **31**, S109 (1997).

[45] T. Sato, J. Plasma Fusion Res. SERIES **2**, 3 (1999).

[46] T. Sato and the Complexity Simulation Group, Prog. Theor. Phys. Supplement **138**, 657 (2000).

Table 1: Potential energy parameters used in our simulation [33].

parameter	value	unit
d_0	0.153	nm
θ_0	1.2310	rad
k_d	70000	kcal/nm^2·mol
k_θ	100	kcal/rad^2·mol
k_ϕ	2.0	kcal/mol
ϵ	0.1984	kcal/mol
σ	0.36239	nm

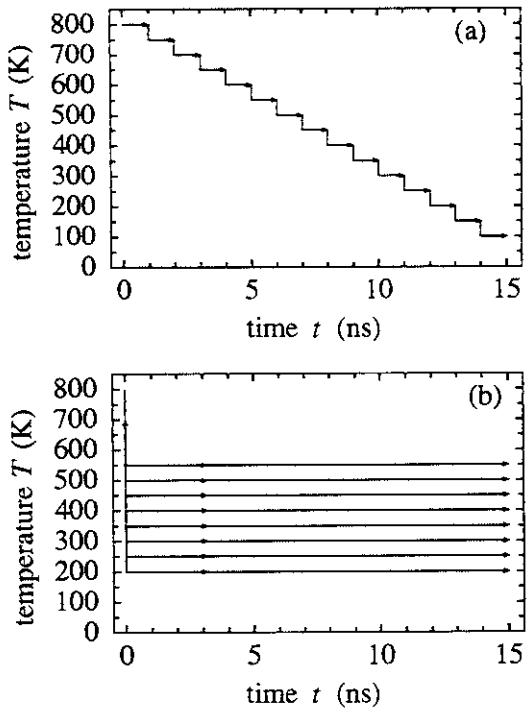

Figure 1: Schematic explanation of the cooling process: (a) gradual stepwise cooling and (b) quenching.

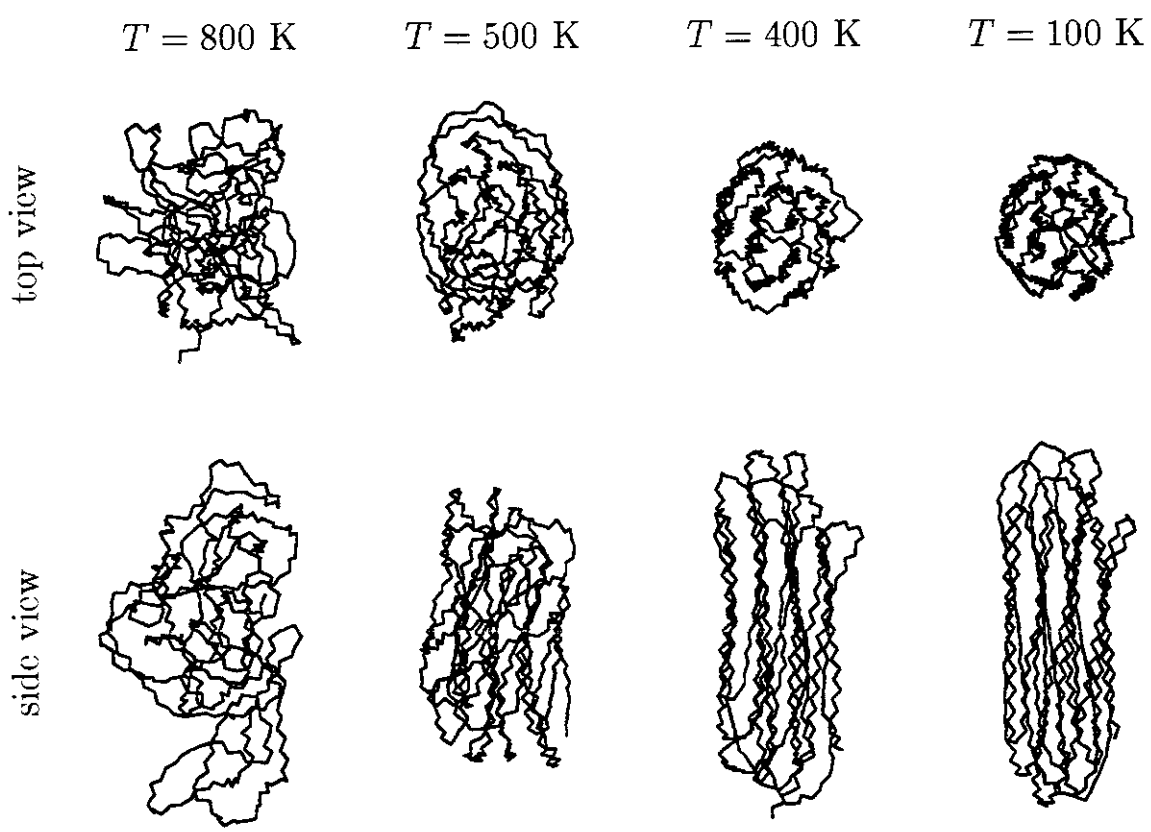

Figure 2: Snapshots of the final chain configuration of a single polymer chain at each temperature: $T = 800$ K, 500 K, 400 K, and 100 K (from left to right) in the case of gradual stepwise cooling. Top and bottom snapshots are respectively viewed along the z-axis (top view) and along the direction perpendicular to the z-axis (side view), where the z-axis is defined as the principal axis with the smallest moment of inertia.

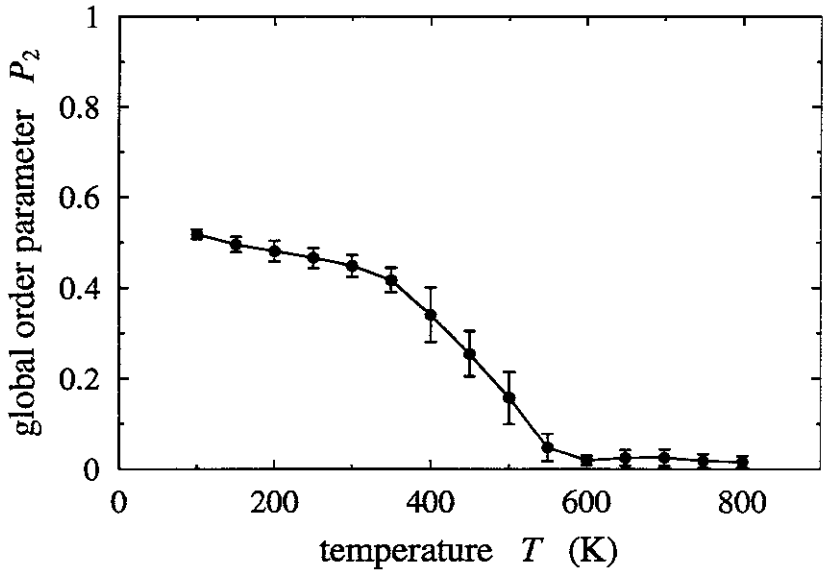

Figure 3: The global orientational order parameter P_2 vs temperature T in the case of gradual stepwise cooling. Time average is taken between 0.2 and 1.0 ns.

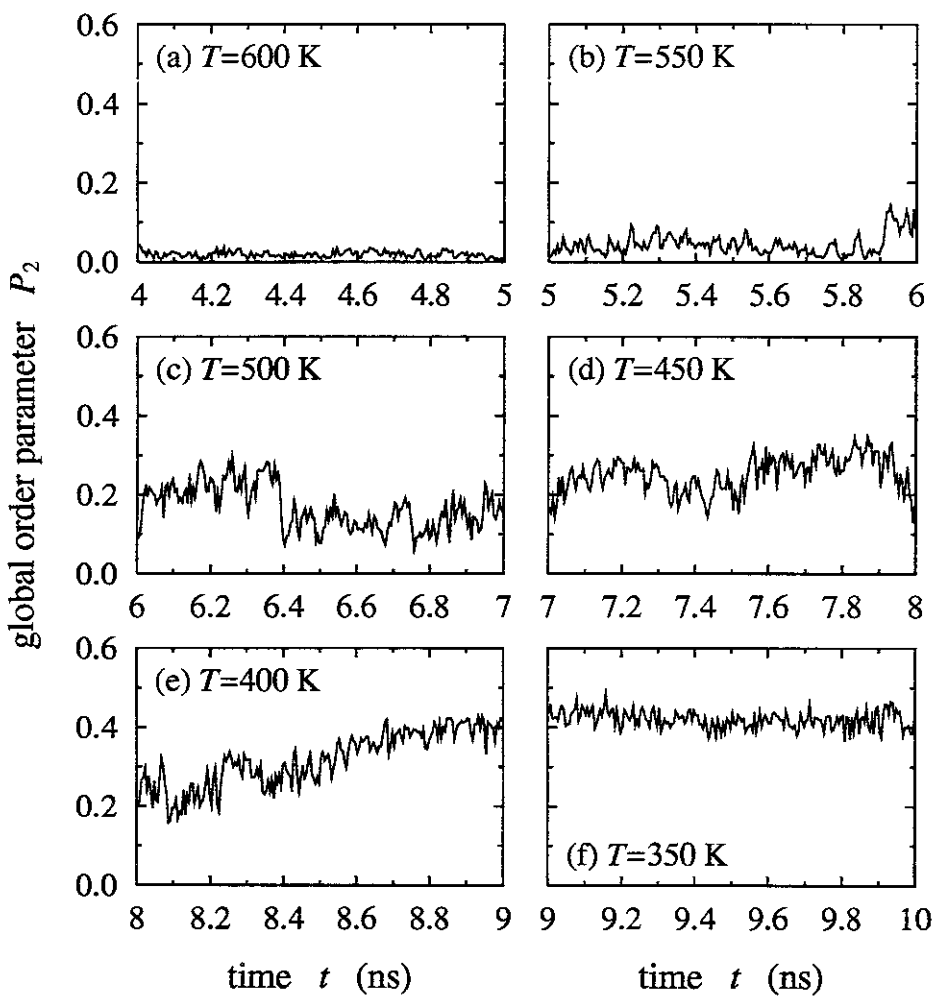

Figure 4: The global orientational order parameter P_2 vs time t (a) at $T = 600$ K, (b) at $T = 550$ K, (c) at $T = 500$ K, (d) at $T = 450$ K, (e) at $T = 400$ K, and (f) at $T = 350$ K in the case of gradual stepwise cooling. Segmental average is taken with $\Delta t = 5$ ps.

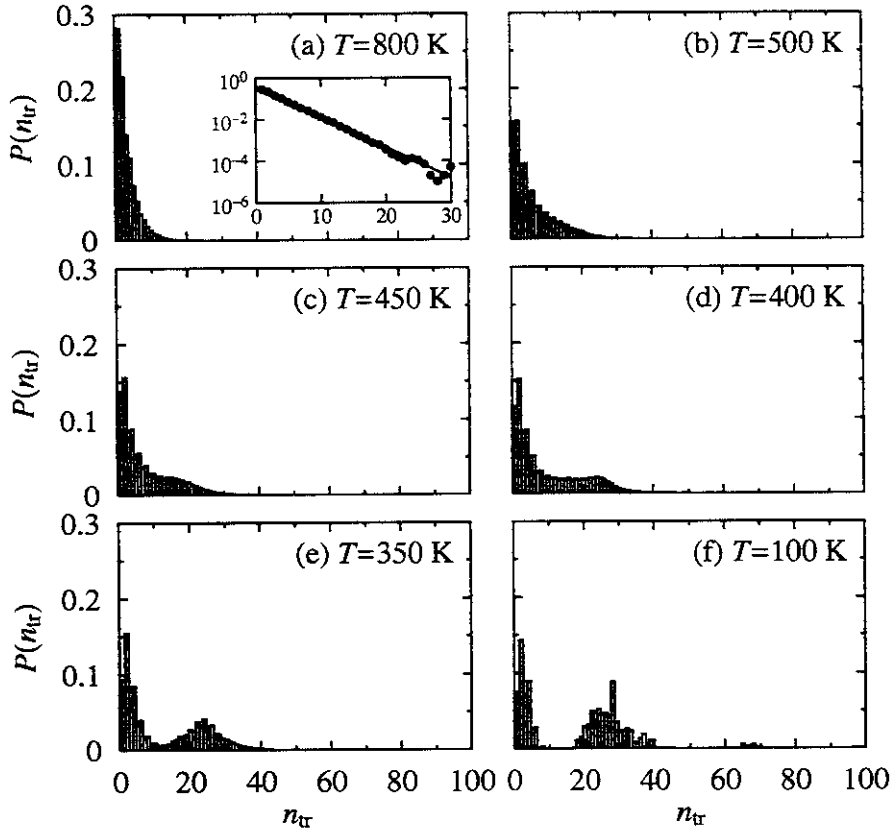

Figure 5: The distribution of the size of the *trans* segments $P(n_{tr})$ averaged between 0.95 and 1.0 ns (a) at $T = 800$ K, (b) at $T = 500$ K, (c) at $T = 450$ K, (d) at $T = 400$ K, (e) at $T = 350$ K, and (f) at $T = 100$ K in the case of gradual stepwise cooling. The inset of (a) is plotted in a linear-log scale.

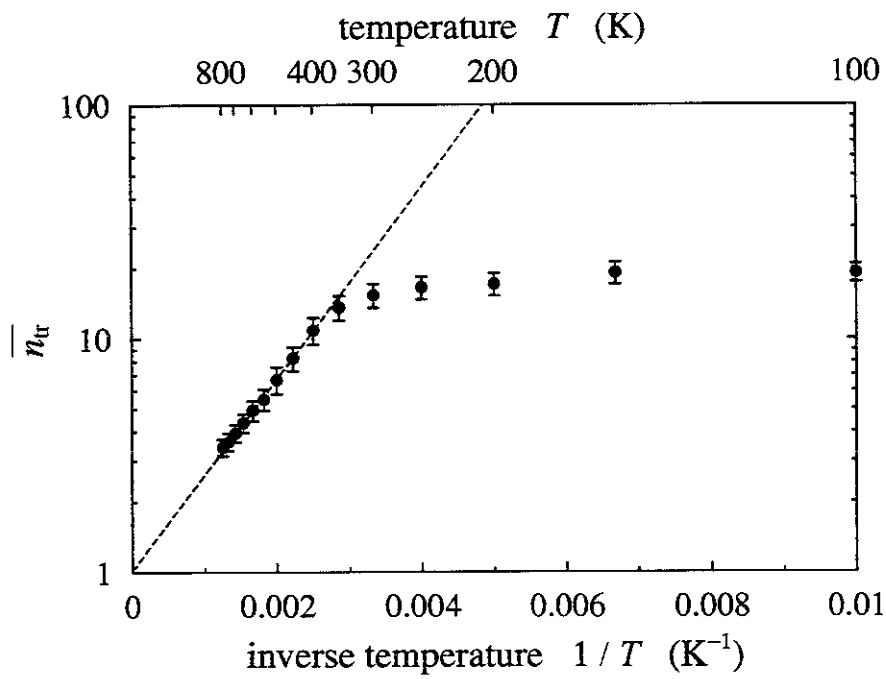

Figure 6: The average size of the *trans* segments $\overline{n_{tr}}$ vs inverse temperature $1/T$ in the case of gradual stepwise cooling. Time average is taken between 0.2 and 1.0 ns. The dashed line represents the line fitted by Eq. (8) with $\Delta\varepsilon/k_B \approx 1.88$ (kcal/mol).

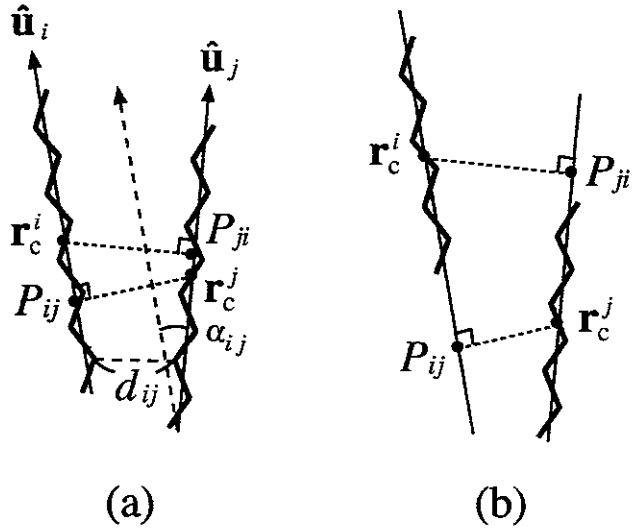

Figure 7: (a) Schematic illustration for the definition of a "*trans* domain". d_{ij} is the shortest distance between the i-th *trans* segment and the j-th *trans* segment, P_{ij} is the foot of a perpendicular drawn from the center of mass of the j-th *trans* segment to the i-th *trans* segment, and α_{ij} is the angle between the principal axis with the smallest moment of inertia of the i-th *trans* segment and that of the j-th *trans* segment. (b) An example of two *trans* segments which do not belong to the same *trans* domain under the second condition.

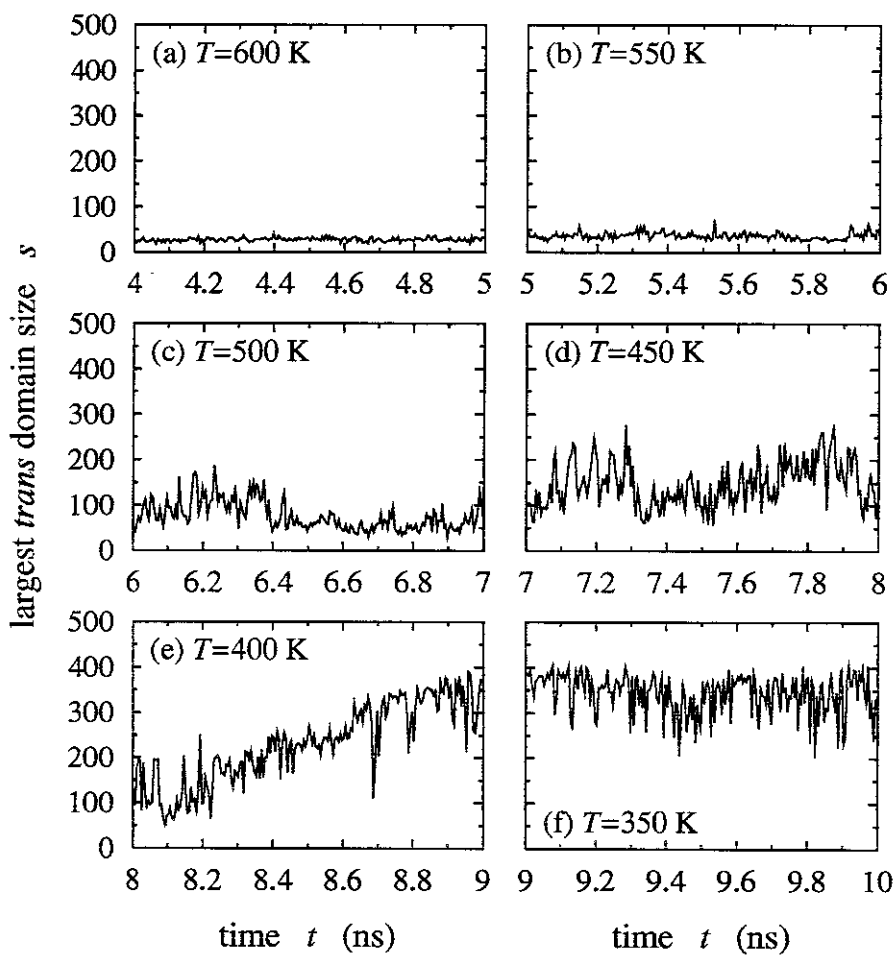

Figure 8: The largest *trans* domain size s vs time t (a) at $T = 600$ K, (b) at $T = 550$ K, (c) at $T = 500$ K, (d) at $T = 450$ K, (e) at $T = 400$ K, and (f) at $T = 350$ K in the case of gradual stepwise cooling. Segmental average is taken with $\Delta t = 5$ ps.

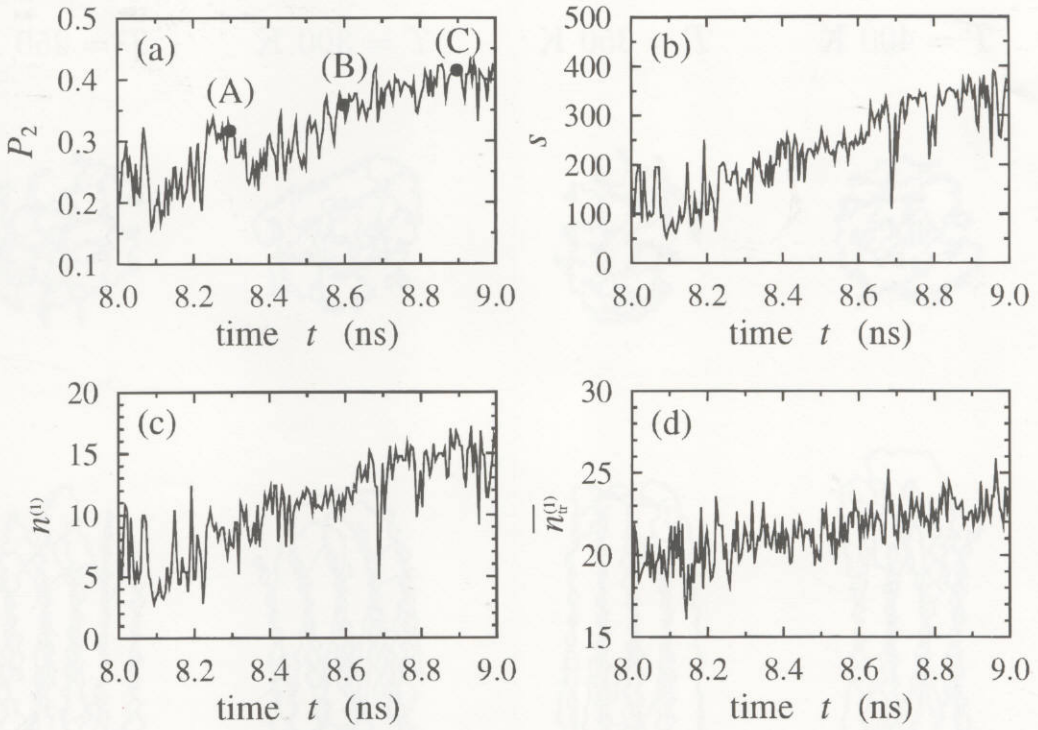

Figure 9: The time evolution of (a) P_2, (b) s, (c) $n^{(1)}$, and (d) $\overline{n_{\rm tr}^{(1)}}$ at $T = 400$ K in the case of gradual stepwise cooling. Segmental average is taken with $\Delta t = 5$ ps. Filled circles (a), (b), and (c) in the figure (a) correspond to $t = 0.3$ ns, 0.6 ns, and 0.9 ns, respectively (See Fig. 10).

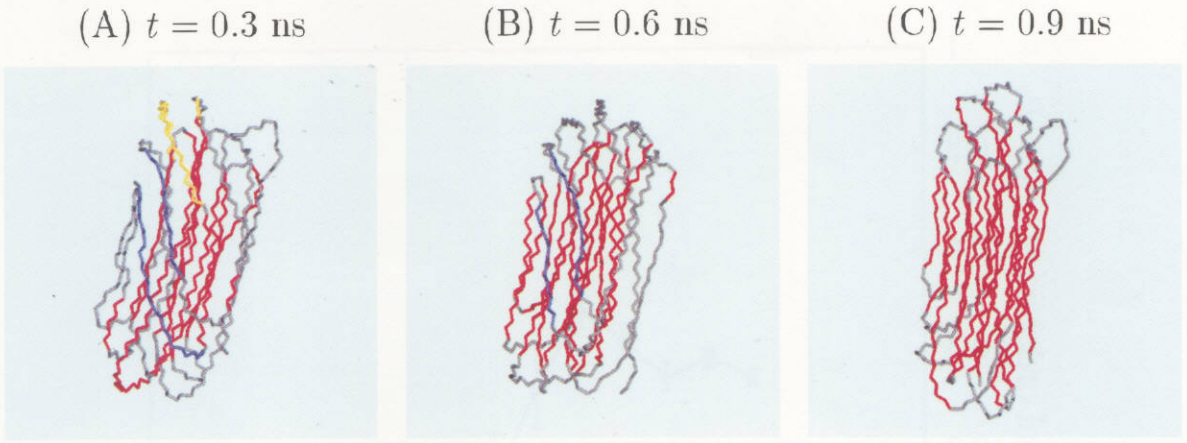

Figure 10: Growth of *trans* domains at $T = 400$ K in the case of gradual stepwise cooling: (a) $t = 0.3$ ns, (b) $t = 0.6$ ns, and (c) $t = 0.9$ ns, which are indicated by filled circles in Fig. 9(a). The largest, the second largest, and the third largest *trans* domains are respectively denoted by red, blue, and yellow colors. Gray denotes *gauche* bonds or small *trans* domains whose sizes are smaller than 30.

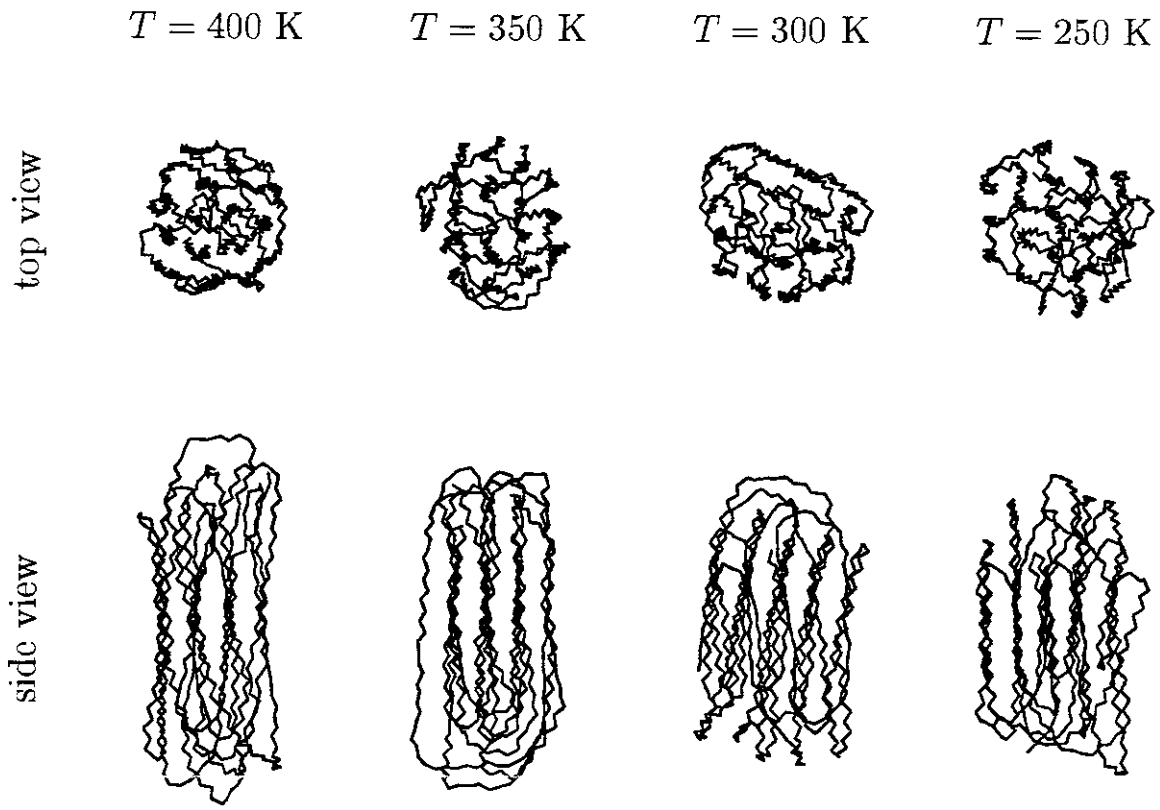

Figure 11: Snapshots of the final chain configuration of a single polymer chain at each temperature: $T = 400$ K, 350 K, 300 K, and 250 K (from left to right) in the case of quenching. Top and bottom snapshots are respectively viewed along the z-axis (top view) and along the direction perpendicular to the z-axis (side view).

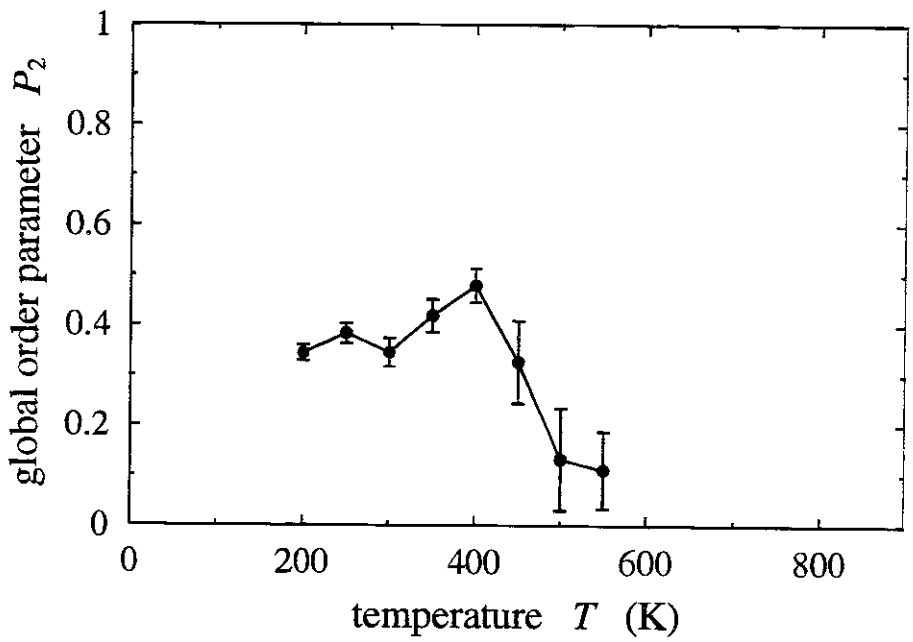

Figure 12: The global orientational order parameter P_2 vs temperature T in the case of quenching. Time average is taken between 5 and 15 ns.

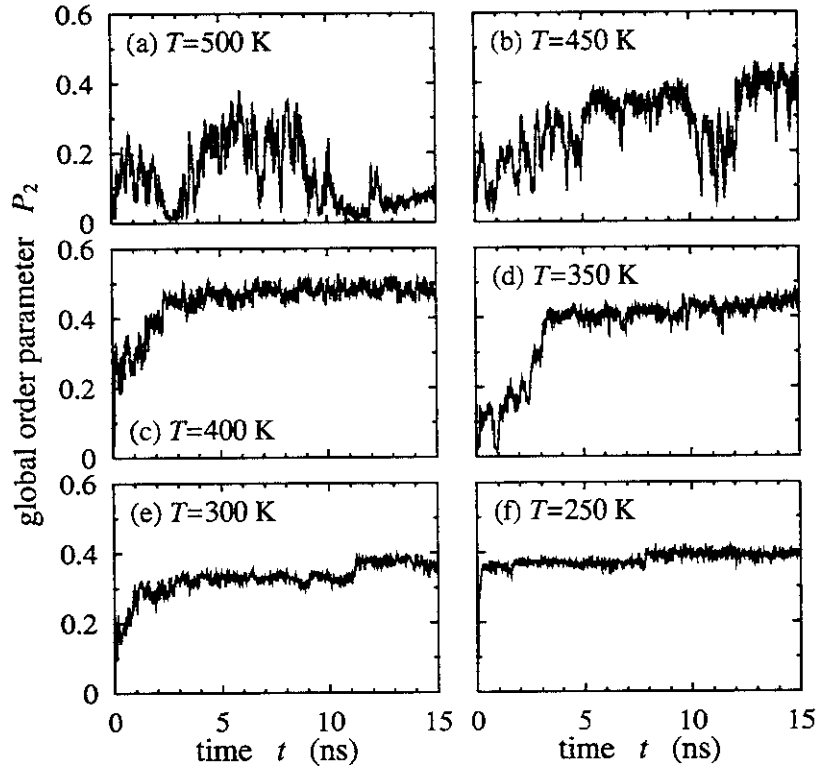

Figure 13: The global orientational order parameter P_2 vs time t (a) at $T = 500$ K, (b) at $T = 450$ K, (c) at $T = 400$ K, (d) at $T = 350$ K, (e) at $T = 300$ K, and (f) at $T = 250$ K in the case of quenching. Segmental average is taken with $\Delta t = 20$ ps.

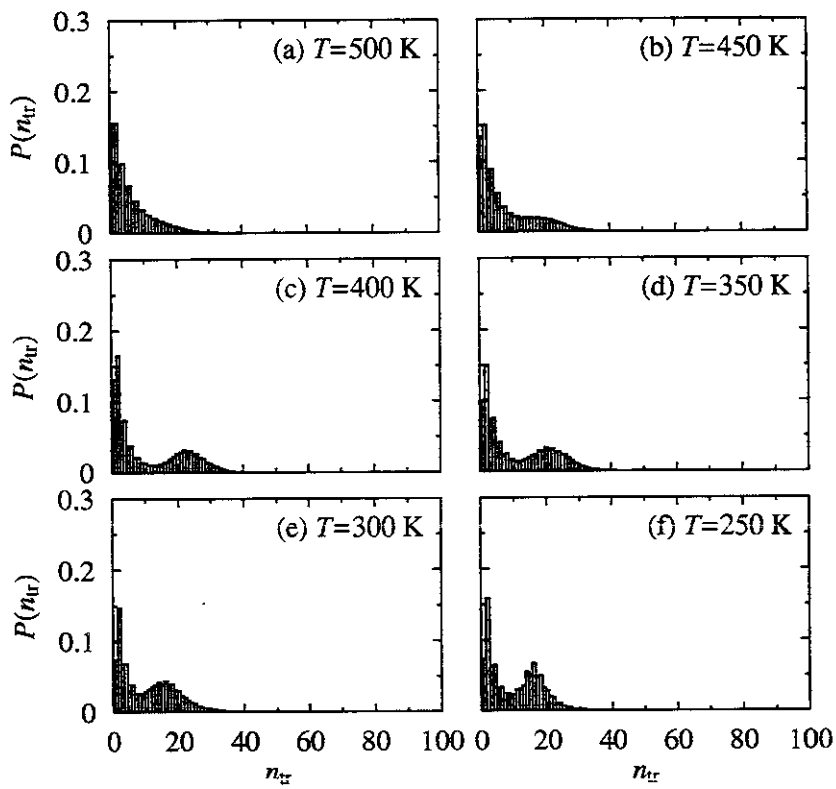

Figure 14: The distribution of the size of the *trans* segments $P(n_{\rm tr})$ averaged between 14 and 15 ns (a) at $T = 500$ K, (b) at $T = 450$ K, (c) at $T = 400$ K, (d) at $T = 350$ K, (e) at $T = 300$ K, and (f) at $T = 250$ K in the case of quenching.

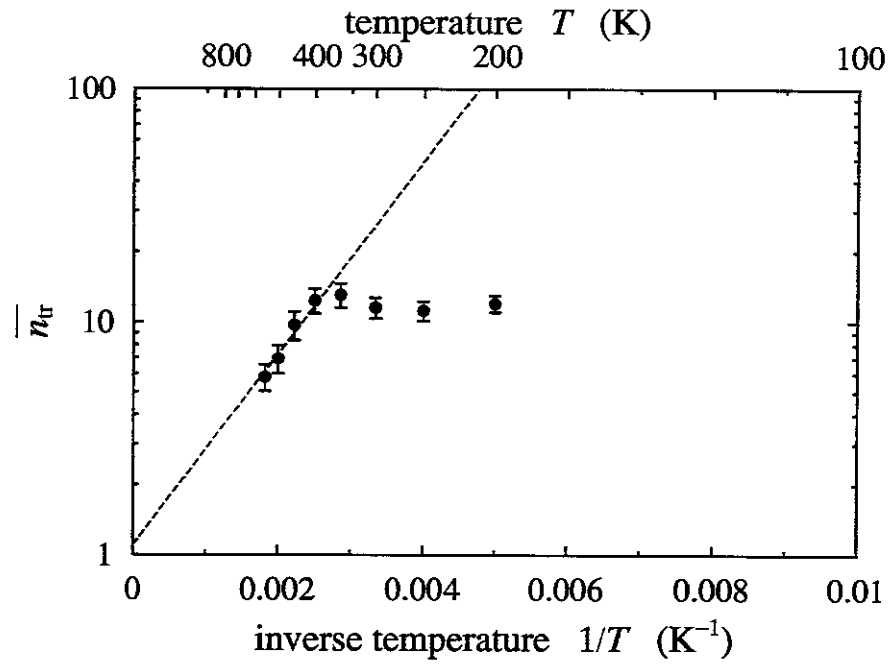

Figure 15: The average size of the *trans* segments $\overline{n_{tr}}$ vs inverse temperature $1/T$ in the case of quenching. Time average is taken between 5 and 15 ns. The dashed line represents the line fitted by Eq. (8) with $\Delta\varepsilon/k_B \approx 1.88$ (kcal/mol).

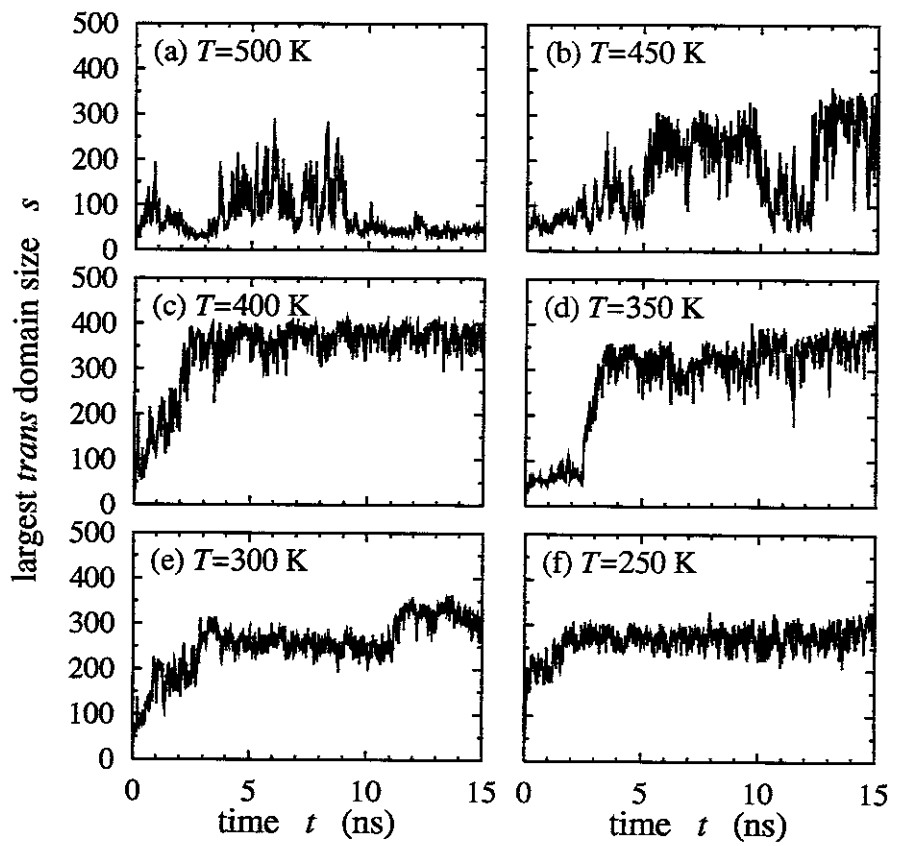

Figure 16: The largest *trans* domain size s vs time t (a) at $T = 500$ K, (b) at $T = 450$ K, (c) at $T = 400$ K, (d) at $T = 350$ K, (e) at $T = 300$ K, and (f) at $T = 250$ K in the case of quenching. Segmental average is taken with $\Delta t = 20$ ps.

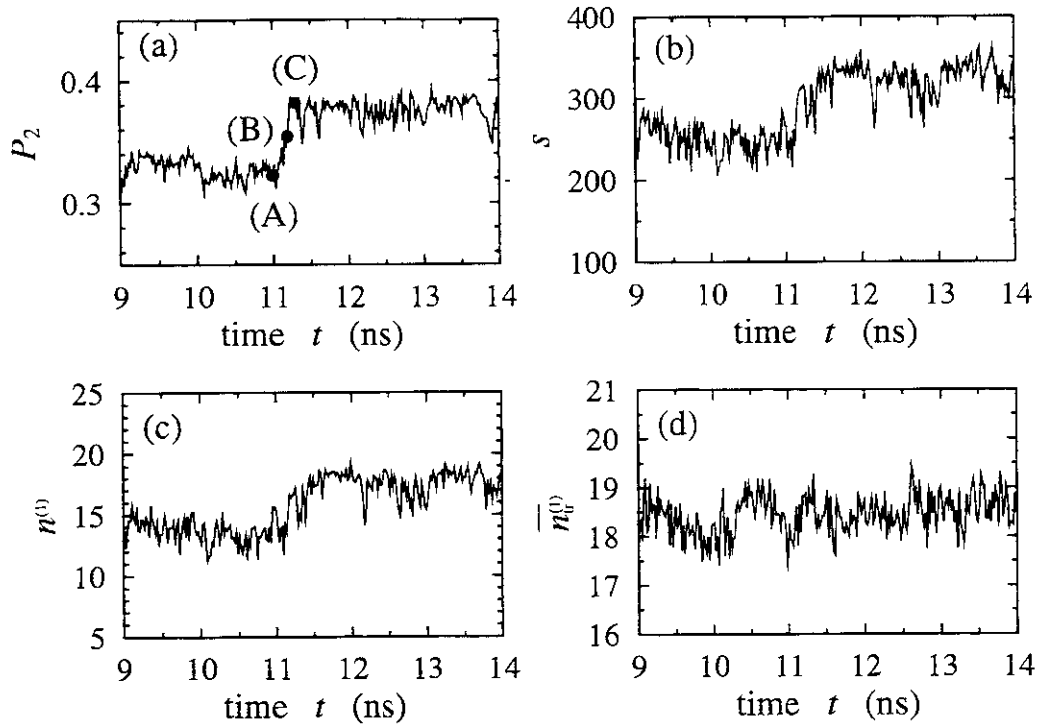

Figure 17: The time evolution of (a) P_2, (b) s, (c) $n^{(1)}$, and (d) $\overline{n_{tr}^{(1)}}$ at $T = 300$ K in the case of quenching. Segmental average is taken with $\Delta t = 20$ ps. Filled circles (a), (b), and (c) in the figure (a) correspond to $t = 11.0$ ns, 11.2 ns, and 11.3 ns, respectively (See Fig. 19).

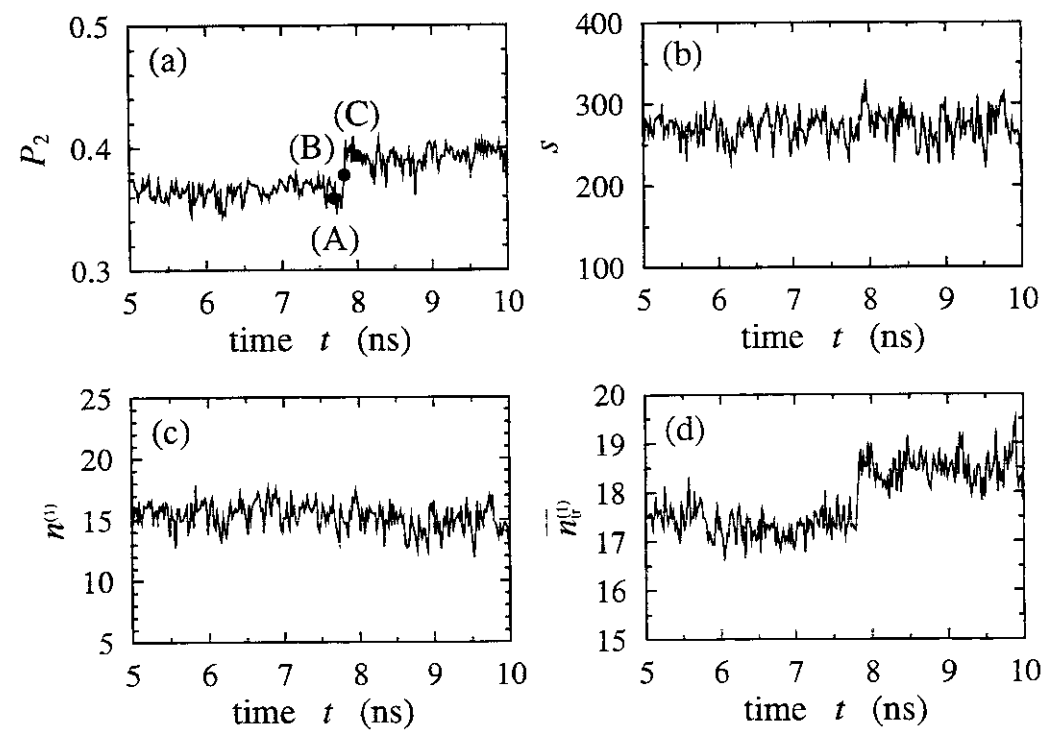

Figure 18: The time evolution of (a) P_2, (b) s, (c) $n^{(1)}$, and (d) $\overline{n_{tr}^{(1)}}$ at $T = 250$ K in the case of quenching. Segmental average is taken with $\Delta t = 20$ ps. Filled circles (a), (b), and (c) in the figure (a) correspond to $t = 7.7$ ns, 8.0 ns, and 9.0 ns, respectively (See Fig. 20).

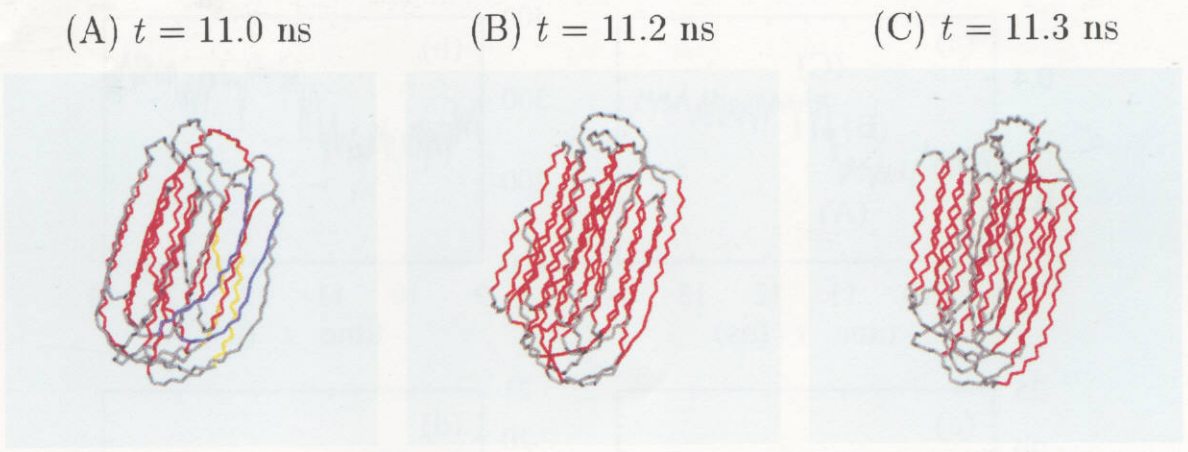

Figure 19: Growth of *trans* domains at $T = 300$ K in the case of quenching: (a) $t = 11.0$ ns, (b) $t = 11.2$ ns, and (c) $t = 11.3$ ns, which are indicated by filled circles in Fig. 17(a). The largest, the second largest, and the third largest *trans* domains are respectively denoted by red, blue, and yellow colors. Gray denotes *gauche* bonds or small *trans* domains whose sizes are smaller than 30.

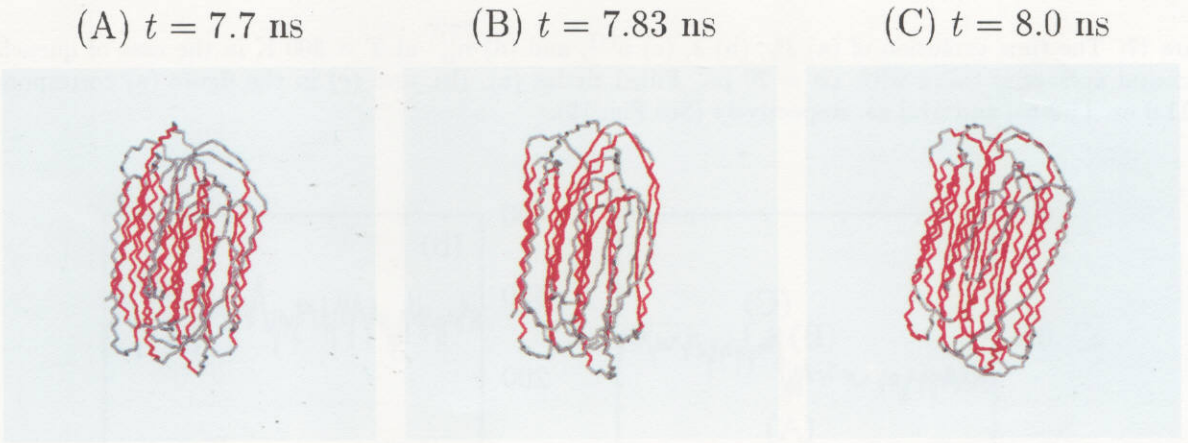

Figure 20: Growth of *trans* domains at $T = 250$ K in the case of quenching: (a) $t = 7.7$ ns, (b) $t = 7.83$ ns, and (c) $t = 8.0$ ns, which are indicated by filled circles in Fig. 18(a). Gray denotes *gauche* bonds or small *trans* domains whose sizes are smaller than 30.

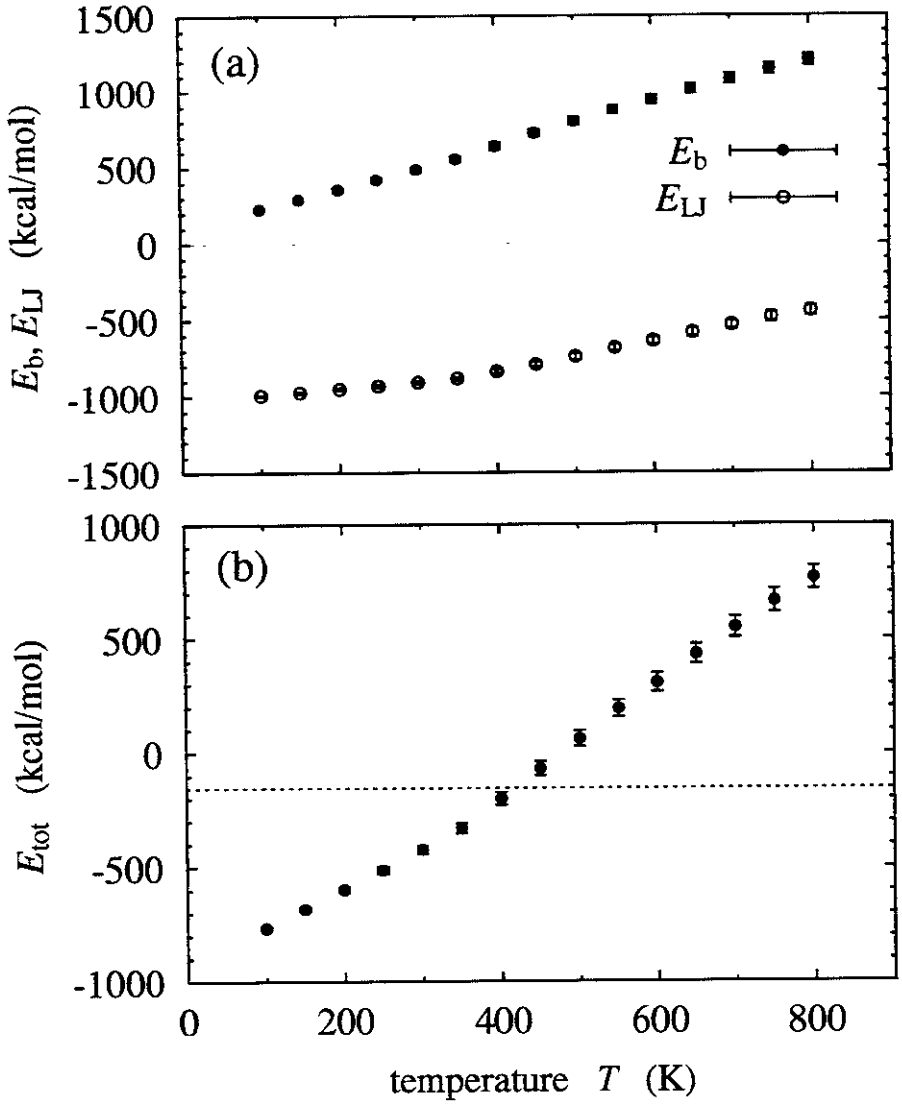

Figure 21: The temperature dependence of (a) the bonded potential energy, E_b, and the Lennard-Jones potential energy, E_{LJ}, and (b) the total potential energy, E_{tot} in the case of gradual stepwise cooling. Time average is taken during the last 0.8 ns. A broken line represents the total potential energy of the all-*trans* conformation

Recent Issues of NIFS Series

NIFS-656 K Narihara, I Yamada, N Ohyabu, K Y Watanabe, N Ashikawa, P C deVries, M Emoto, H Funaba, M Goto, K Ichiguchi, K Ida, H Idei, K Ikeda, S Inagaki, N Inoue, K Isobe, S Kado, O Kaneko, K Kawahata, K Khlopenkov, TKobuchi, A Komori, S Kubo, R Kumazawa, Y Liang, TMasuzaki, I Minami, J Miyazawa, I Morisaki, S Morita, S Murakami, S Muto, I Mutoh, Y Nagayama, Y Nakamura, H Nakanishi, Y Narushima, K Nishimura, N Noda, TNotake, S Ohdachi, Y Oka, M Osakabe, S Ozaki, R O Pavlichenko, B J Peterson, A Sagara, K Saito, S Sakakibara, R Sakamoto, H Sasao, M Sasao, K Sato, M Sato, TSeki, TShimozuma, C Shoji, H Suzuki, A Takayama, M Takechi, Y Takeiri, N Tamura, K Tanaka, K Toi, N Tokuzawa, Y Torii, K Tsumori, T Watari, H Yamada, S Yamaguchi, S Yamamoto, M Yokoyama, Y Yoshimura, S Satow, K Itoh, K Ohkubo, K Yamazaki, S Sudo, O Motojima, Y Hamada, M Fujiwara,
Transition from Ion Root to Electron Root in NBI Heated Plasmas in LHD Sep 2000
(IAEA-CN-77/EXP5/28)

NIFS-657 M Sasao, S Murakami, M Isobe, A V Krasilnikov, S Iiduka, K Itoh, N Nakajima, M Osakabe, K Saito, I Seki, Y Takeiri, T Watari, N Ashikawa, P deVaries, M Emoto, H Funaba, M Goto, K Ida, H Idei, K Ikeda, S Inagaki, N Inoue, S Kado, O Kaneko, K Kawahata, K Khlopenkov, TKobuchi, A Komori, S Kubo, R Kumazawa, S Masuzaki, TMinami, J Miyazawa, TMorisaki, S Morita, S Muto, TMutoh, Y Nagayama, Y Nakamura, H Nakanishi, K Narihara, K Nishimura, N Noda, TNotake, Y Liang, S Ohdachi, N Ohyabu, Y Oka, TOzaki, R O Pavlichenko, B J Peterson, A Sagara, S Sakakibara, R Sakamoto, H Sasao4, K Sato, M Sato, I Shimozuma, M Shoji, H Suzuki, M Takechi, N Tamura, K Tanaka, K Toi, TTokuzawa, Y Torii, K Tsumori, H Yamada, I Yamada, S Yamaguchi, S Yamamoto, M Yokoyama, Y Yoshimura, K Y Watanabe and O Motojima,
Study of Energetic Ion Transport in the Large Helical Device Sep 2000
(IAEA-CN-77/EX9/1)

NIFS-658 B J Peterson, Y Nakamura, K Yamazaki, N Noda, J Rice, Y Takeiri, M Goto, K Narihara, K Tanaka, K Sato, S Masuzaki, S Sakakibara, K Ida, H Funaba, M Shoji, M Osakabe, M Sato, Yuhong Xu, TKobuchi, N Ashikawa, P deVries, M Emoto, H Idei, K Ikeda, S Inagaki, N Inoue, M Isobe, S Kado, K Khlopenkov, S Kubo, R Kumazawa, TMinami, J Miyazawa, TMorisaki, S Murakami, S Muto, TMutoh, Y Nagayama, H Nakanishi, K Nishimura, TNotake, Y Liang, S Ohdachi, YOka, TOzaki, R O Pavlichenko, A Sagara, K Saito, R Sakamoto, H Sasao, M Sasao, TSeki, TShimozuma, H Suzuki, M Takechi, N Tamura, K Toi, TTokuzawa, Y Torii, K Tsumori, I Yamada, S Yamaguchi, S Yamamoto, M Yokoyama, Y Yoshimura, K Y Watanabe, T Watari, K Kawahata, O Kaneko, N Ohyabu, H Yamada, A Komori, S Sudo, O Motojima
Impurity transport induced oscillations in LHD Sep 2000
(IAEA-CN-77/EXP5/27)

NIFS-659 T Satow, S Imagawa, N Yanagi, K Takahata, T Mito, S Yamada, H Chikaraishi, A Nishimura, I Ohtake, Y Nakamura, S Satoh, O Motojima,
Achieved Capability of the Superconducting Magnet system for the Large Helical Device Sep 2000
(IAEA-CN-77/FTP1/15)

NIFS-660 T Watari, T Mutoh, R Kumazawa, T Seki, K Saito, Y Torii, Y P Zhao, D Hartmann, H Idei, S Kubo, K Ohkubo, M Sato, T Shimozuma, Y Yoshimura, K Ikeda, O Kaneko, Y Oka, M Osakabe, Y Takeiri, K Tsumori, N Ashikawa, P C deVries, M Emoto, A Fukuyama, H Funaba, M Goto, K Ida, S Inagaki, N Inoue, M Isobe, K Itoh, S Kado, K Kawahata, T Kobuchi, K Khlopenkov, A Komori, A Krasilnikov, Y Liang, S Masuzaki, K Matsuoka, T Minami, J Miyazawa, T Morisaki, S Morita, S Murakami, S Muto, Y Nagayama, Y Nakamura, H Nakanishi, K Narihara, K Nishimura, N Noda, A TNotake, S Ohdachi, N Ohyabu, H Okada, M Okamoto, T Ozaki, R O Pavlichenko, B J Peterson, A Sagara, S Sakakibara, R Sakamoto, H Sasao, M Sasao, K Sato, S Satoh, T Satow, M Shoji, S Sudo, H Suzuki, M Takechi, N Tamura, S Tanahashi, K Tanaka, K Toi, T Tokuzawa, K Y Watanabe, T Watanabe, H Yamada, I Yamada, S Yamaguchi, S Yamamoto, K Yamazaki, M Yokoyama, Y Hamada, O Motojima, M Fujiwara,
The Performance of ICRF Heated Plasmas in LHD, Sep 2000
(IAEA-CN-77/EX8/4)

NIFS-661 K Yamazaki, K Y Watanabe, A Sagara, H Yamada, S Sakakibara, K Narihara, K Tanaka, M Osakabe, K Nishimura, O Motojima, M Fujiwara, the LHD Group
Helical Reactor Design Studies Based on New Confinement Scalings Sep 2000
(IAEA-CN-77/ FTP 2/12)

NIFS-662 T Hayashi, N Mizuguchi, H Miura and T Sato,
Dynamics of Relaxation Phenomena in Spherical Tokamak Sep 2000
(IAEA-CN-77THP2/13)

NIFS-663 H Nakamura and T Sato, H Kambe and K Sawada and T Saiki
Design and Optimization of Tapered Structure of Near-field Fiber Probe Based on FDTD Simulation Oct 2000

NIFS-664 N Nakajima,
Three Dimensional Ideal MHD Stability Analysis in $L=2$ Heliotron Systems Oct 2000

NIFS-665 S Fujiwara and T Sato,
Structure Formation of a Single Polymer Chain I Growth of trans Domains Nov 2000